

CORRELATION BETWEEN POLYMER PACKING AND GAS TRANSPORT PROPERTIES FOR CO₂/N₂ SEPARATION IN GLASSY FLUORINATED POLYIMIDE MEMBRANE

P. C. TAN¹, Z. A. JAWAD², B. S. OOI¹, A. L. AHMAD¹, S. C. LOW^{1,*}

¹School of Chemical Engineering, Engineering Campus, Universiti Sains Malaysia, Seri Ampangan, 14300 Nibong Tebal, Pulau Pinang, Malaysia

²Department of Chemical Engineering, School of Engineering and Science, Curtin University Sarawak Campus, 250 CDT, 98009 Miri, Sarawak, Malaysia

*Corresponding Author: chsclow@usm.my

Abstract

Gas separation performance of a membrane highly hinges on its physical properties. In this study, the interplay between polymer packing of a membrane and its gas transport behaviours (permeability and selectivity) was investigated through a series of 6FDA-DAM:DABA (3:2) polyimide membranes with different polymer compactness. The chemical structure and the polymer packing of the resulting membrane were characterized using attenuated total reflectance-Fourier transform infrared spectroscopy (ATR-FTIR) and packing density measurement, respectively. CO₂/N₂ separation efficiency of the membrane was evaluated at 25°C with feed pressure up to 6 bar. N₂ permeability was found to rely on the membrane's packing density, which signified its greater dependence on molecular sieving. In contrast, sorption showed a more vital role in determining the CO₂ permeability. In this work, the membrane with a final thickness of 97±2 µm had successfully surpassed the Robeson's 2008 upper bound plot with a CO₂ permeability of 83 Barrer and CO₂/N₂ selectivity of 97 at 3 bar permeation.

Keywords: Packing density, Free volume, Gas transport properties, CO₂/N₂ separation, fluorinated polyimide.

1. Introduction

Membrane-based gas separation has emerged as one of the fastest growing branches of separation technology for replacement or use in combination with the traditional gas separation techniques such as amine absorption [1, 2]. The

aromatic polyimide, with better separation efficiency than conventional cellulose acetate and polysulfone membrane [3], had emerged as the potential candidate for promising gas separation membrane. Besides the excellent inherent chemical resistance, aromatic polyimide also possesses high thermal stability, good mechanical strength and easy processing for high performance gas separation modules [4].

As for gas separation, it is apparent that the gas diffusivity and solubility are of important factors affecting gas transport. The major physicochemical factors influencing polymer gas permeability and selectivity includes: (i) the polymer-penetrant interactions, (ii) the inter-segmental spacing that represents the mean free polymer volume, and (iii) the condensability of the penetrant [5, 6]. Present work focused on the inter-segmental spacing and the condensability of the penetrant in a pristine polyimide membrane.

Many efforts have been made to discuss how to decrease packing density of the polymers and how to gain a larger quantity of free spaces between the polymer neighbouring segments. It is well-known that gas permeability of a polymer becomes larger by decreasing the polymer packing density or increasing the membrane free volume [7]. Indeed, the fractional free volumes increase with looser packing of segment; as a result, the diffusivity will be increased [5, 7]. In present work, with the introduction of the bulky-C(CF₃)₂- bridging group in 4, 4'-(hexafluoroisopropylidene) diphthalic anhydride (6FDA) moiety, the fluorinated polyimide is tends to restrict the torsional motion of the polymer chains and a higher free volume can be obtained [8]. Hence, a membrane with higher productivity is anticipated. Meanwhile, 3,5-diaminobenzoic acid (DABA diamine) which can provide acid sites for crosslinking reaction [9] is also incorporated into the polyimide backbone, aiming to enhance the membrane plasticization resistance.

The ultimate aim of this work is to study the relationship between the polymer free volume and the gas penetrant solubility in an aromatic polyimide membrane, 6FDA-DAM:DABA (3:2). The packing density and free volume of the fluorinated polyimide membranes were adjusted through the conformation of the polymers in different polymer dope volume. A thicker cast-film is expected to provide a larger free space environment for the rearrangement of the polymeric molecular chains to achieve a favourable low entropy configuration. The conformation of the polymers in solution was believed to affect the packing of the polymer chains in the membrane and further affect the gas transport behaviour of CO₂ and N₂. Present work provides an in-depth insight into the underlying membrane's physical features-performance correlation, which serves as a pivotal understanding for the development of the decent pristine polyimide membrane for ensuing research.

2. Materials and Methods

The following subsections will provide the details of the materials used in polymer synthesis and flat sheet membrane fabrication. Different methods used in characterizing membrane properties will also be described in detail.

2.1. Materials

Monomers for polyimide synthesis constituted of 4,4'- (hexafluoroisopropylidene) diphthalic anhydride (6FDA, 99% purity), 2, 4, 6-trimethyl-m-phenylenediamine (DAM, 96% purity) and 3, 5-diaminobenzoic acid (DABA, 98% purity) were purchased from Sigma-Aldrich. 1-methyl-2-pyrrolidinone (NMP, 99.5% purity), acetic anhydride (dehydrating agent, 99% purity) and triethylamine (catalyst, > 99 % purity) used for polymer synthesis were attained from Sigma-Aldrich (Germany), Acros Organics (Belgium) and Sigma-Aldrich (Belgium) respectively. Methanol used for polymer precipitation was obtained from Merck (Germany). For the membrane fabrication, tetrahydrofuran (Fisher Scientific, UK) was used as solvent. Gases (CO₂, N₂) used in the permeation test were supplied by Wellgas (Malaysia), with a purity of >99%. All the chemicals were used as received without further purification.

2.2. Polymer synthesis

The polyimide polymer was synthesized through two-step reactions, namely polycondensation and cyclodehydration. Since the reaction is water sensitive, all monomers were dried under vacuum at 40°C to remove trapped moisture. First, diamines DAM:DABA with a molar ratio of 3:2 were dissolved in NMP at ambient temperature under nitrogen purging. Stoichiometric amount of 6FDA was then added portionwise into the diamines solution to produce 20 wt% solution. The solution was stirred for 24 h under inert atmosphere to form polyamic acid and latter converted to polyimide through chemical imidization with the addition of equimolar acetic anhydride and triethylamine. Continuous stirring was performed for another 24 h. The polyimide polymer was precipitated from the viscous solution and washed for several times using methanol. The precipitated polyimide was then filtered and air-dried in the fume hood for 16 h followed by vacuum drying at 200°C for 24 h to complete the chemical imidization.

2.3. Membrane formation and thermal treatment

Specific volume of the polyimide solution (10 wt.% polyimide dissolved in THF) was poured on a glass petri dish placed inside the glove box. The glove box was saturated with THF solvent to promote slow phase inversion. After two days of solvent evaporation, the membrane was removed and dried at 180°C under vacuum for 24 h to eliminate any residual solvent. The volume of polyimide solution was varied (ranging from 1.54 mL to 5 mL, which correspond to initial membrane thickness of 400 µm to 1300 µm) to attain membrane with different compactness. The membrane formed was then thermally treated using a dual zone split tube furnace (MTI-OTF-1200X-80-II, USA) to induce decarboxylation crosslinking. The tube furnace was purged with nitrogen prior to the thermal treatment and the nitrogen purge was maintained at 80 mL/min throughout the process. The thermal treatment protocol comprised of heating from room temperature to 330 °C at a ramping rate of 5 °C/min, followed by a gentle heating rate of 1 °C/min to 370 °C. After 1 h of dwelling at 370 °C, the membrane was cooled down to room temperature in the furnace.

2.4. Membrane characterization

Thermo Scientific Fourier transform infrared spectrometer (ATR-FTIR, NICOLET iS10, USA) was utilized to confirm complete imidization of the polyimide polymer. Measurement was conducted over wavenumber range of 4000-525 cm^{-1} with spectral resolution of 4 cm^{-1} and 16 scans.

Membrane sample was cut into a dimension of 1 cm x 1 cm and its thickness, l (μm) was recorded. The membrane sample was dried in oven at 40 $^{\circ}\text{C}$ for 10 minutes. The heating step was repeated until a constant weight of dried membrane, W (g) was obtained. The packing density was then calculated:

$$\rho \left(\frac{\text{g}}{\text{cm}^3} \right) = \frac{10000W}{Al} \quad (1)$$

where A is the area of the membrane sample (cm^2).

Single gas permeation test was carried out to investigate gas transport properties of the membrane. The permeation test was conducted in a membrane cell with effective membrane area of 7.07 cm^2 . Steady state permeability and selectivity were assessed at 25 $^{\circ}\text{C}$ with feed pressure up to 6 bar. Prior to the permeation test, the whole system was thoroughly purged with purified nitrogen to eliminate humid vapour. The permeate flow rate was measured with a bubble flow meter at atmospheric pressure. Gas permeability was calculated based on the permeate flow rate:

$$P = \frac{\dot{V}pl}{T A \Delta p} \times 2695.93 \quad (2)$$

where P is the gas permeability in Barrer (1 Barrer = 1 $\times 10^{-10}$ $\text{cm}^3(\text{STP})$ $\text{cm}/\text{cm}^2 \text{ s cmHg}$), \dot{V} is the permeate flow rate (cm^3/s), p represents the downstream pressure (Pa), l signifies the membrane thickness (μm), T refers to the operating temperature (K), A denotes the effective membrane area (cm^2) and Δp symbolizes the differential pressure (cmHg). The ideal selectivity, α_{AB} for gases A and B is defined as the ratio of their permeability. The permeation test was repeated for several times and the average permeability and selectivity were reported.

3. Results and Discussion

During the course of polymerization, polyimide polymer was produced by reacting polyamic acid intermediate with an amide functional group through chemical imidization. To ensure the functionality of the polymer used for membrane fabrication, ATR-FTIR technique was employed to characterize chemical structure of the polymer synthesized. As shown in Fig. 1, FTIR spectrum of the synthesized polyimide polymer showed the characteristic absorption bands of polyimide near 1785 cm^{-1} and 1725 cm^{-1} which were associated with the stretching vibration of C=O symmetrically and asymmetrically respectively. Besides, the asymmetric C-N stretching that representing the aromatic polyimide ring was ascertained at 1350 cm^{-1} . A strong and sharp peak was also observed around 720 cm^{-1} , which verified the bending of imide ring present in polyimide. In contrast, typical bands of the polyamic acid at 1650 cm^{-1} (C=O vibration frequency) and 1550 cm^{-1} (N-H bending vibration) were not found in the synthesized polymer. Instantly, it indicated that the

synthesized polyimide polymer was fully imidized with the conversion of all amide groups into the imide functional group.

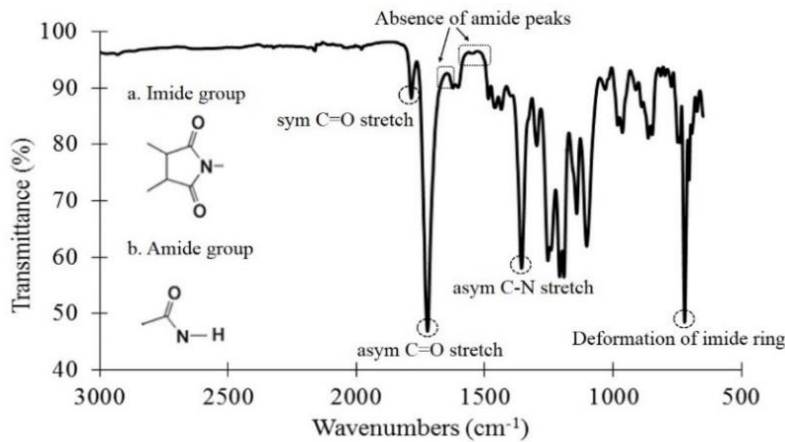


Fig. 1. FTIR spectrum of 6FDA-DAM:DABA (3:2) polymer.

In dense film gas separation, the permeation mechanism is best described by solution-diffusion process where the diffusivity and solubility of gas penetrant were the main concerns. It is mentioned that gas diffusivity is interrelated to the packing of polymer chains as well as the size and shape of penetrant [5]. Hence, the compactness of the membrane is crucial in determining the separation efficiency for specific gas pairs. In view of that, packing density which reflects the compactness of the membrane synthesized was examined to have a detailed understanding on the membrane's gas transport behaviour. As summarized in Table 1, 16% increase in packing density was observed when the initial membrane thickness was increased from 400 μm ($1.12 \pm 0.05 \text{ g/cm}^3$) to 700 μm ($1.30 \pm 0.11 \text{ g/cm}^3$). However, the increasing rate of membrane compactness was slowed down, with only 5.4% increment in packing density, when the initial membrane thickness was further increased to 1300 μm ($1.37 \pm 0.05 \text{ g/cm}^3$). With the increase of initial cast-film thickness (or higher volume of the casting dope), more polyimide molecules were eventually involved in film solidification. As the THF solvent evaporated out from the membrane, the higher content of the polyimide molecules in the thicker membrane were tended to attract each other with increasing cohesive forces of polymers [10, 11], which resulted in compactness of intermolecular free spaces, as tabulated in Table 1. Moreover, the membrane's compactness could also be inferred from the final membrane thickness. Theoretically, membrane is considered to have same polymer packing if the thickness ratio of both initial casting thickness (1300 $\mu\text{m}/400 \mu\text{m}$) and final formed thickness (97 $\mu\text{m}/32 \mu\text{m}$) were comparable. A thickness ratio of 3.03 was calculated from the membranes' final thicknesses; whilst, thickness ratio of 3.25 was accounted for membranes' initial thicknesses. This indicated that the final thickness of the 1300 μm membrane was thinner than predicted, which denoted a more highly packed structure of the polymer matrix.

Table 1. Summary for membrane characterization.

Initial membrane thickness (μm)	Volume of input polymer solution (mL)	Final membrane thickness (μm)	Packing density (g/cm^3)
400	1.54	32 ± 2	1.12 ± 0.05
700	2.69	60 ± 4	1.30 ± 0.11
1000	3.85	72 ± 3	1.30 ± 0.01
1300	5.00	97 ± 2	1.37 ± 0.05

As aforementioned, different packing density of the polymer matrix could manipulate the diffusivity of gas penetrant, which in turn affects the gas permeability for a particular membrane. As depicted in Fig. 2, N_2 permeability decreased in a thicker membrane, conforming to the increasing packing density of the membrane, as showed in Table 1. A membrane with higher packing density implied a more compact film, where the molecular sieving effect was magnified for the bigger gas penetrant such as N_2 . Indeed, N_2 was found to have insignificant solubility as compared to CO_2 [7, 12], reflecting the permeability of N_2 was governed mainly by diffusion. The bigger size N_2 molecule (3.64 \AA) is expected to demonstrate slower diffusion than that of smaller size CO_2 (3.3 \AA). Thus, in present work, a greater molecular sieving resistance for the transport of N_2 was anticipated for membrane with higher packing density and hence restricted the N_2 mobility across the film. A considerable 72% decline in N_2 permeability was revealed when the final membrane thickness increased from $32\pm 2 \mu\text{m}$ to $60\pm 4 \mu\text{m}$ (Table 1), which corresponded to the initial membrane thickness of $400 \mu\text{m}$ and $700 \mu\text{m}$ respectively. It was followed by a gentle decrease of N_2 permeability when the final membrane thickness was further increased to $97\pm 2 \mu\text{m}$ (corresponded to initial thickness of $1300 \mu\text{m}$). The decreasing trend of N_2 permeability was in well accordance to the variation in the membrane compactness, as only a small increment in packing density was found between the membranes with initial casting thickness of $700 \mu\text{m}$ and $1300 \mu\text{m}$. Furthermore, the N_2 permeabilities were comparable for a specific final membrane thickness, although the feed pressure was increased from 2 bar to 6 bar (Fig. 2). This signified that the sorption played a minor role in defining N_2 permeability as the solubility of N_2 in polyimide matrix was insignificant.

On the contrary, diverging trend was demonstrated by the permeability of carbon dioxide (CO_2). Fig. 3 displays that the CO_2 permeability increased when a thicker membrane was used for gas separation. 1.75 times larger of CO_2 permeability was recorded when the final membrane thickness was increased from $32\pm 2 \mu\text{m}$ (86 Barrer) to $97\pm 2 \mu\text{m}$ (151 Barrer) at 1 bar. The level of sorption for a specific penetrant is highly dependent on the free volume in the polymeric membrane [5]. In glassy polyimide membrane, the non-equilibrium nature of polymer created unrelaxed free volumes [13], especially through the introduction of the bulky substituent CF_3 in present work. Although the cast-films demonstrated a slight increase of the polymer density (Table 1), however, the increased of the membranes' final thicknesses has speculated the formation of more polymer conformation layers within the polymer matrix; thus, more apparent "free spaces" were anticipated in the final formed membrane. However, the pre-existed unrelaxed free space will reduced through physical aging, a process of polymer structure relaxation which resulted in polymer matrix

densification [14]. It was generally accepted that the physical aging process was accelerated in thin film compared to the thicker film [13]. Therefore, with the slower physical aging process and higher apparent free volume in the thicker membrane, the membrane provided more “free” spacing for Langmuir sorption of CO_2 , leading to higher permeability, which was consistent with the permeation results in Fig. 3.

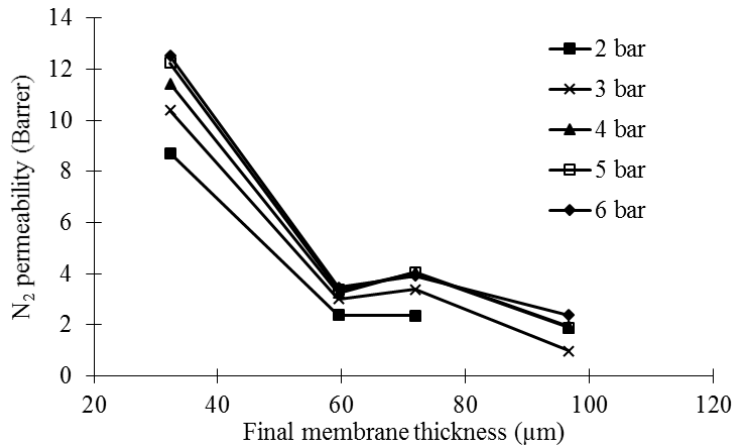


Fig. 2. N_2 permeability for membranes with different final thickness.

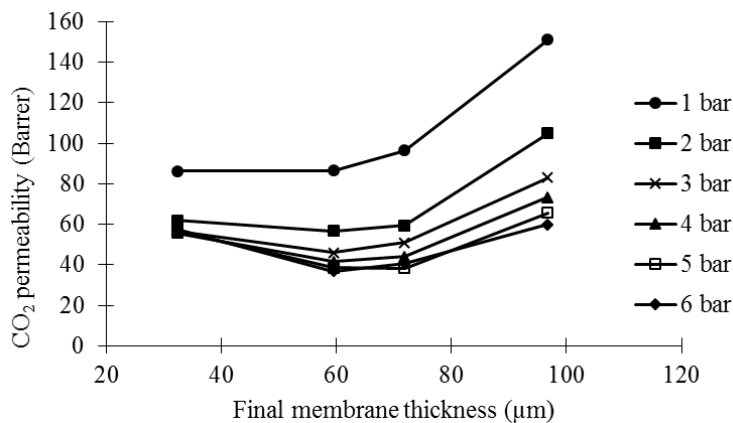


Fig. 3. CO_2 permeability for membranes with different final thickness.

On the aspect of the penetrant condensability in a polymer matrix, the CO_2 , which comprises higher critical temperature of 304.2 K than N_2 (126.1 K), showed greater condensability and solubility in the polyimide membrane. In a study carried out by Scholes and co-workers [12], Langmuir affinity constant of N_2 in the Matrimid membrane is 6.8 times lower than CO_2 . Under different polymer–gas interaction (polyimide- CO_2 and polyimide- N_2), the polyimide membrane is expected to exhibit higher CO_2 solubility than N_2 [7]. Hence, it is

believed that sorption is more influential compared to diffusivity in impacting the CO₂ permeability, causing dissimilar trend from N₂ permeability in Fig. 2.

The higher sorption capacity of a thicker membrane was verified in Fig. 4. A sharper decline of CO₂ permeability was reported with increasing feed pressure in a thicker membrane (97±2 μm). Indeed, the sharper decline of the CO₂ permeability reflected the higher availability of the Langmuir sorption sites (higher free volume) in the membrane [13, 15]. For a glassy polymer, such as polyimide, sorption is explained by the dual mode sorption behaviours, namely Langmuir mode sorption (hole filling of pre-existed free volume) and Henry's mode sorption (dissolution of penetrant to the densely packed region of polymer) [15]. At lower pressure, Langmuir mode sorption dominates as the gas penetrants were preferentially filled into the microvoids with lower energy sorption sites [16], which are also known as the free volume existed in the membrane matrix. Principally, Langmuir mode sorption is described by two parameters, i.e. Langmuir affinity constant and Langmuir capacity constant. The Langmuir affinity constant is correlated to the penetrant condensability, where CO₂ was showed to have a higher affinity constant in the polyimide matrix than N₂ [12]. On the other hand, the Langmuir capacity constant defines the maximum amount of penetrants that are able to be sorbed into the polymer matrix, which was directly related to the quantity of the free volume created in the membrane [17]. The role of Langmuir sorption is overtaken by Henry's mode of sorption at higher pressure due to the saturation of the Langmuir sites [18]. As a whole, the solubility coefficient reduces with increasing pressure attributed to the saturation of Langmuir sites, promoted the reduction of CO₂ permeability at the higher pressure (Fig. 4). Therefore, a sharper decrement in CO₂ permeability for the thicker membrane (97±2 μm) in Fig. 4 reflected a faster filling of Langmuir sites and stronger CO₂ sorption. Hence, it can be deduced that the increase of CO₂ permeability (Fig. 3) in a thicker membrane was mainly dedicated to the higher CO₂ sorption in the polyimide matrix.

Apart from permeability, permselectivity is also an important parameter to characterize the functionality of a membrane. Since there is always a trade-off between membrane permeability and permselectivity, Robeson's trade-off curve, which provides guidance in evaluation of membrane practicability, was utilized to assess the membrane separation performances. From the literatures, the CO₂/N₂ separation capabilities for most of the polyimide membranes were still lying under the Robeson's 2008 upper bound curve. As highlighted in Fig. 5, the separation performances of the membranes synthesized in this work were moderate and comparable with the documented literature data. Despite not all of the membranes synthesized could surpass the Robeson's 2008 polymer upper bound curve, the membrane with final thickness of 97 ±2 μm had successfully transcended the trade-off curve at 3 bar of permeation test (25°C). It achieved a CO₂ permeability of 83 Barrer with superior CO₂/N₂ selectivity of 97. In fact, Robeson's upper bound plot could be surmounted in the work by just synthesizing the pristine polyimide membrane; implies the enormous potential and practicability of the polyimide polymer for gas separation. A more promising separation performances are within realms of possibility with further exploitation of the pristine polyimide membrane, for instance development of the mixed matrix membrane [19].

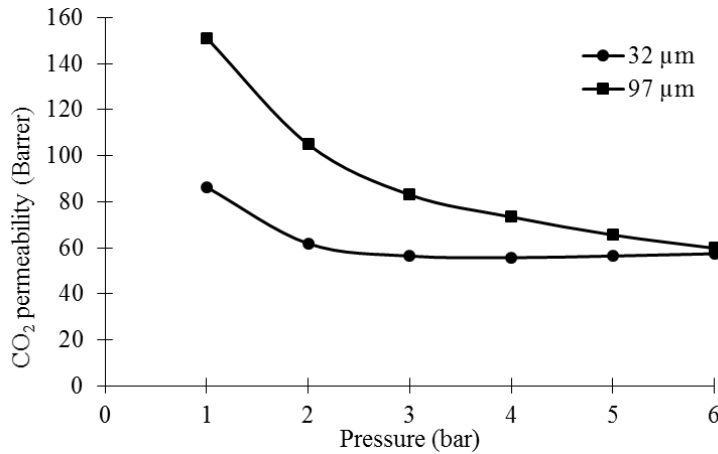


Fig. 4. Decline of CO₂ permeability due to dual mode sorption.

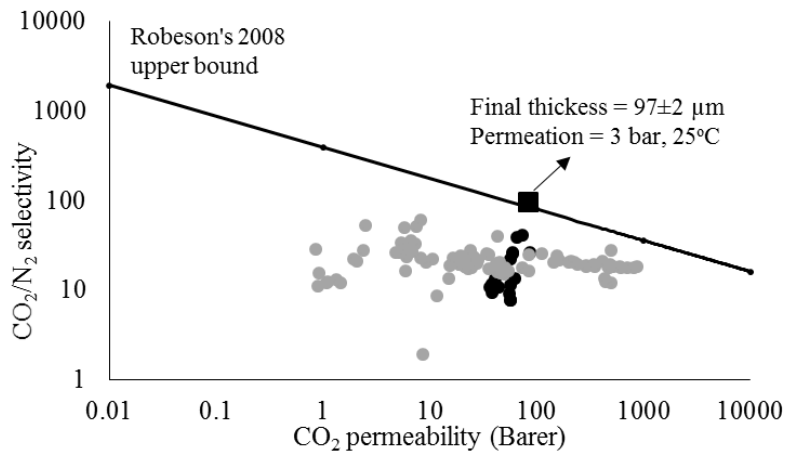


Fig. 5. Robeson's 2008 upper bound curve for CO₂/N₂ separation. The black colour dots represented the separation performance of membranes in this work while the grey colour dots referred the polyimide membrane separation data obtained from literatures (Robeson plot from [20]; data from [4, 9, 21-34]).

4. Conclusions

Fluorinated 6FDA-DAM:DABA (3:2) polyimide membranes with various polymer compactness were successfully fabricated via dry phase inversion. In this study, the role of membrane's physical properties was inter-related to its gas separation performances. With insignificant sorption behaviour of N₂ in polyimide matrix, N₂ permeability was mainly governed by molecular sieving effect, where the overall permeability has been restricted by the thicker membrane with higher packing density. On the other hand, sorption was found to be more influential in impacting the CO₂ permeability. It was believed that the slower physical aging of thicker membrane

provided more apparent free spacing for CO₂ Langmuir sorption, resulting in an increasing trend of CO₂ permeability with the increased of the membrane thickness. The membrane with final thickness of 97±2 µm, which corresponded to packing density of 1.37±0.05 g/cm³, was found in the commercially attractive region of the Robeson's 2008 upper bound plot with superior CO₂/N₂ permselectivity of 97 and 83 Barrer of CO₂ permeability at 3 bar. In regards, the polyimide membrane synthesized in current work illustrated enormous potential and practicability to achieve promising gas separation membrane.

Acknowledgment

The authors wish to thank the financial support granted by Long Term Research Grant Scheme (LRGS) (304/PJKIMIA/6050296/U124). All authors are affiliated to the Membrane Science and Technology Cluster of USM. P. C. Tan is financially assisted by the Human Life Advancement Foundation (HLAF) Scholarships.

References

1. Wang, Y.-C.; Huang, S.-H.; Hu, C.-C.; Li, C.-L.; Lee, K.-R.; Liaw, D.-J.; and Lai, J.-Y. (2005). Sorption and transport properties of gases in aromatic polyimide membranes. *Journal of Membrane Science*, 248, 15-25.
2. Mohamed, F.; Hasbullah, H.; Jamian, W.N.R.; Rani, A.R.A.; Saman, W.N.H.W.; Salleh, W.; and Ismail, A.F. (2015). Morphological investigation of poly(lactic acid) asymmetric membrane. *Journal of Engineering Science and Technology*, 10 (special issue 2), 1-8.
3. Bos, A.; Pünt, I.G.M.; Wessling, M.; and Strathmann, H. (1998). Plasticization-resistant glassy polyimide membranes for CO₂/CO₄ separations. *Separation and Purification Technology*, 14(1), 27-39.
4. Maya, E.M.; Tena, A.; de Abajo, J.; de La Campa, J.G.; and Lozano, A.E. (2010). Partially pyrolyzed membranes (PPMs) derived from copolyimides having carboxylic acid groups. Preparation and gas transport properties. *Journal of Membrane Science*, 349(1), 385-392.
5. Wind, J.D.; Sirard, S.M.; Paul, D.R.; Green, P.F.; Johnston, K.P.; and Koros, W.J. (2003). Carbon dioxide-induced plasticization of polyimide membranes: pseudo-equilibrium relationships of diffusion, sorption, and swelling. *Macromolecules*, 36(17), 6433-6441.
6. Tsvigu, C.; Pavesi, E.; De Angelis, M.; and Baschetti, M.G. (2015). Effect of relative humidity and temperature on the gas transport properties of 6FDA–6FpDA polyimide: Experimental study and modelling. *Journal of Membrane Science*, 485, 60-68.
7. Hirayama, Y.; Yoshinaga, T.; Kusuki, Y.; Ninomiya, K.; Sakakibara, T.; and Tamari, T. (1996). Relation of gas permeability with structure of aromatic polyimides I. *Journal of Membrane Science*, 111, 169-182.
8. Neyertz, S.; Brown, D.; Pandiyan, S.; and van der Vegt, N.F. (2010). Carbon dioxide diffusion and plasticization in fluorinated polyimides. *Macromolecules*, 43(18), 7813-7827.

9. Qiu, W.; Chen, C.-C.; Xu, L.; Cui, L.; Paul, D.R.; and Koros, W.J. (2011). Sub- T_g cross-linking of a polyimide membrane for enhanced CO₂ plasticization resistance for natural gas separation. *Macromolecules*, 44(15), 6046-6056.
10. Hiemenz, P.C. (1977). *Principles of Colloid and Surface Chemistry (3rd ed.)*. M. Dekker.
11. Lii, J.H. ; and Allinger, N.L. (1989). Molecular mechanics. The MM3 force field for hydrocarbons. 3. The van der Waals' potentials and crystal data for aliphatic and aromatic hydrocarbons. *Journal of the American Chemical Society*, 111(23), 8576-8582.
12. Scholes, C.A.; Tao, W.X.; Stevens, G.W.; and Kentish, S.E. (2010). Sorption of methane, nitrogen, carbon dioxide, and water in Matrimid 5218. *Journal of Applied Polymer Science*, 117(4), 2284-2289.
13. Xia, J.; Chung, T.-S.; and Paul, D.R. (2014). Physical aging and carbon dioxide plasticization of thin polyimide films in mixed gas permeation. *Journal of Membrane Science*, 450, 457-468.
14. Huang, Y.; Wang, X.; and Paul, D.R. (2006). Physical aging of thin glassy polymer films: Free volume interpretation. *Journal of Membrane Science*, 277(1), 219-229.
15. Fuhrman, C.; Nutt, M.; Vichtovonga, K.; and Coleman, M.R. (2004). Effect of thermal hysteresis on the gas permeation properties of 6FDA-based polyimides. *Journal of Applied Polymer Science*, 91(2), 1174-1182.
16. Mark, H.F. (2013). *Encyclopedia of Polymer Science and Technology, Concise (3rd ed.)*. John Wiley & Sons.
17. Li, N.N.; Fane, A.G.; Ho, W.W.; and Matsuura, T. (2011). *Advanced Membrane Technology and Applications*. John Wiley & Sons.
18. Zhou, C.; Chung, T.-S.; Wang, R.; Liu, Y.; and Goh, S.H. (2003). The accelerated CO₂ plasticization of ultra-thin polyimide films and the effect of surface chemical cross-linking on plasticization and physical aging. *Journal of Membrane Science*, 225, 125-134.
19. Kusworo, T.; Ismail, A.F.; and Mustafa, A. (2015). Experimental design and response surface modeling of PI/PES-Zeolite 4A mixed matrix membrane for CO₂ separation. *Journal of Engineering Science and Technology*, 10(9), 1116-1130.
20. Robeson, L.M. (2008). The upper bound revisited. *Journal of Membrane Science*, 320(1), 390-400.
21. Kim, J.H.; Koros, W.J.; and Paul, D.R. (2006). Effects of CO₂ exposure and physical aging on the gas permeability of thin 6FDA-based polyimide membranes: Part 2. with crosslinking. *Journal of Membrane Science*, 282(1), 32-43.
22. Kanehashi, S.; Kishida, M.; Kidesaki, T.; Shindo, R.; Sato, S.; Miyakoshi, T.; and Nagai, K. (2013). CO₂ separation properties of a glassy aromatic polyimide composite membranes containing high-content 1-butyl-3-methylimidazolium bis (trifluoromethylsulfonyl) imide ionic liquid. *Journal of Membrane Science*, 430, 211-222.
23. Chua, M.L.; Xiao, Y.; and Chung, T.-S. (2014). Using iron (III) acetylacetonate as both a cross-linker and micropore former to develop

- polyimide membranes with enhanced gas separation performance. *Separation and Purification Technology*, 133, 120-128.
24. Lua, A.C.; and Shen, Y. (2013). Preparation and characterization of polyimide–silica composite membranes and their derived carbon–silica composite membranes for gas separation. *Chemical Engineering Journal*, 220, 441-451.
 25. Kammakakam, I.; Yoon, H.W.; Nam, S.; Park, H.B.; and Kim, T.-H. (2015). Novel piperazinium-mediated crosslinked polyimide membranes for high performance CO₂ separation. *Journal of Membrane Science*, 487, 90-98.
 26. Wang, S.; Tian, Z.; Feng, J.; Wu, H.; Li, Y.; Liu, Y.; Li, X.; Xin, Q.; and Jiang, Z. (2015). Enhanced CO₂ separation properties by incorporating poly (ethylene glycol)-containing polymeric submicrospheres into polyimide membrane. *Journal of Membrane Science*, 473, 310-317.
 27. Lively, R.P.; Dose, M.E.; Xu, L.; Vaughn, J.T.; Johnson, J.R.; Thompson, J.A.; Zhang, K.; Lydon, M.E.; Lee, J.-S.; Liu, L.; Hu, Z.; Karvan, O.; Realf, M.J.; and Koros, W.J. (2012). A high-flux polyimide hollow fiber membrane to minimize footprint and energy penalty for CO₂ recovery from flue gas. *Journal of Membrane Science*, 423, 302-313.
 28. Tanaka, K.; Okano, M.; Toshino, H.; Kita, H.; and Okamoto, K.I. (1992). Effect of methyl substituents on permeability and permselectivity of gases in polyimides prepared from methyl-substituted phenylenediamines. *Journal of Polymer Science Part B: Polymer Physics*, 30(8), 907-914.
 29. Yamamoto, H.; Mi, Y.; Stern, S.A.; and St Clair, A.K. (1990). Structure/permeability relationships of polyimide membranes. II. *Journal of Polymer Science Part B: Polymer Physics*, 28(12), 2291-2304.
 30. Stern, S.A.; Liu, Y.; and Feld, W. (1993). Structure/permeability relationships of polyimides with branched or extended diamine moieties. *Journal of Polymer Science Part B: Polymer Physics*, 31(8), 939-951.
 31. Tanaka, K.; Kita, H.; Okano, M.; and Okamoto, K.-I. (1992). Permeability and permselectivity of gases in fluorinated and non-fluorinated polyimides. *Polymer*, 33(3), 585-592.
 32. Liu, Y.; Chng, M.L.; Chung, T.-S.; and Wang, R. (2003). Effects of amidation on gas permeation properties of polyimide membranes. *Journal of Membrane Science*, 214(1), 83-92.
 33. Stern, S.A.; Mi, Y.; Yamamoto, H.; and Clair, A.K.S. (1989). Structure/permeability relationships of polyimide membranes. Applications to the separation of gas mixtures. *Journal of Polymer Science Part B: Polymer Physics*, 27(9), 1887-1909.
 34. Kim, T.-H.; Koros, W.J.; and Husk, G.R. (1989). Temperature effects on gas permselection properties in hexafluoro aromatic polyimides. *Journal of Membrane Science*, 46, 43-56.